

BIOSONAR-INSPIRED SOURCE LOCALIZATION IN LOW SNR

Sasha Apartsin¹, Leon N. Cooper² and Nathan Intrator¹

¹*Blavatnik School of Computer Science, Tel-Aviv University, Tel-Aviv, Israel*

²*Institute For Brain and Neural Systems and Physics Department, Brown University, Providence, U.S.A.*
{Apartzin, nin}@tau.ac.il, leon_cooper@brown.edu

Keywords: Biosonar, Underground exploration, Threshold effect, Source localization, Time of arrival.

Abstract: Some mammals use sound signals for communications and navigation in the air (bats) or underwater (dolphins). Recent biological discovery shows that blind mole rat is capable of detecting and avoiding underground obstacles using reflection from seismic signals. Such a remarkable capacity relies on the ability to localize the source of the reflection with high accuracy and in very low Signal to Noise Ratio (SNR) conditions. The standard methods for source localization are usually based on Time of Arrival (ToA) estimation obtained by the correlation of received signal with a matched filter. This approach suffers from rapid deterioration in the accuracy as SNR level falls below certain threshold value: the phenomenon known in the Radar Theory as a “threshold effect”. In this paper we describe biosonar-inspired method for ToA estimation and 2D source localization based on the fusion of the measurements from biased estimators which are obtained using a family of unmatched filters. Suboptimal but not perfectly correlated estimators are combined together to produce a robust estimator for ToA and 2D source position which outperforms standard matched filter-based estimator in high noise. The proposed method can be applied for mapping of underground instalments using low power infrasound pulses.

1 INTRODUCTION

Echolocation, also called Biosonar, is the biological sonar used by several mammals such as bats, dolphins and whales. Echolocating animals emit calls out to the environment, and listen to the echoes of those calls that return from various objects in the environment. They use these echoes to locate, range, and identify the objects. Echolocation is used for navigation and for foraging (or hunting) in various environments.

It has been recently discovered (Kimchi et al., 2005) that the blind mole rat uses sonar-like exploration of the underground. This rat, which lives underground and has no functioning eyes, generates ground stimulation by banging its head on the wall of its tunnels.

Mole rat can dig a tunnel 300ft long in one night while detecting and avoiding voids and obstacles (e.g. stones) that are several feet ahead.

The tunnels of mole rats can reach a length of two miles and a mole rat runs inside the tunnel at a thus indicating that it can “see” quite well, although

its eyes are not functioning. From behavioural studies, we learn that a mole rat finds out if some intruder got into its tunnel very quickly (as they become very aggressive).

It thus follows; that the mole rat can utilize its infrasound exploration device to a long range of over a mile. How are the ping returns being transformed into an image, we do not quite know, but one can expect that the mechanism is similar to the one employed by Bats, Dolphins and other biosonar animal. However, in the case of blind mole rat, the transmitted seismic pulse has low central frequency or otherwise it will be quickly absorbed by the soil.

Analysis of signals from returned pings is used extensively in seismic underground exploration. The method requires a controlled seismic source of energy, such as dynamite, a specialized air gun or vibrators, commonly known by their trademark name Vibroseis. These seismic sources produce high energy pulses to ensure high Signal to Noise Ratio at receivers. Obviously, the energy of the explosion is nowhere comparable to the power of pulses generated by blind mole rat.

This work was supported in part by the U.S. Army Research Office

The typical analysis of returned signal involves correlation of the returned signal with a matched filter. The matched filter approach suffers from rapid deterioration in the sensing accuracy as SNR level falls below certain threshold value; the phenomenon known in the Radar Theory as a “threshold effect” (Woodward, 1953).

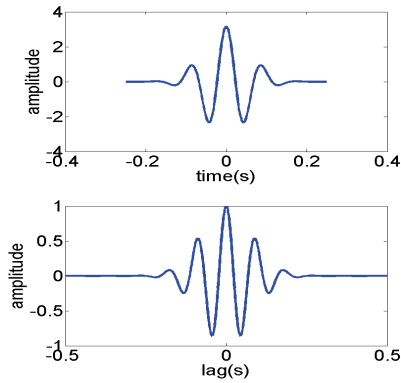


Figure 1: Gaussian modulated sinusoidal pulse (top) and its autocorrelation function $y(t)$.

According to Woodward who studied the threshold effect back in 1953, it is “one of the most interesting features of radar theory”. It appears that when SNR at a receiver falls below certain threshold value, the mean square error of the estimation rapidly increases, causing dramatic drop in sensing accuracy. A receiver operating with SNR above this threshold value is said to be in a coherent state. The matched filter-based estimator is usually used for the coherent receiver. For the SNR levels substantially below the threshold value, a receiver said to be noncoherent with the assumption that most of the information about the pulse carrier phase is lost due to the noise. For in-between levels of SNR, a receiver is said to be a semi-coherent receiver, balancing between coherent and noncoherent states.

The threshold effect is intensified (i.e. occurs at higher SNR levels) as pulse central frequency is reduced. Therefore the conventional matched filter approach might not be the best choice for the processing of responses from low-power low-frequency pulses.

In this paper, we describe a robust single pulse ToA estimation method for semi-coherent receiver. We show how to construct a family of suboptimal and biased estimators, using phase-shifted versions of source waveform as unmatched filters. The outcomes of estimators are fused together into a single ToA estimator, which outperforms conventional Matched Filter (MF) based estimator for a range of low SNR levels.

The same idea can be applied to the problem of 2D source localization, provided matched features have complex reflection cross-section. In 2D case, a family of unmatched filters can be generated from the feature’s template using phase shift in several directions. The increased number of degrees of freedom (phase shift directions) results in even larger improvement in the accuracy.

One of the possible applications for the described method involves detection and mapping of the underground installments by low-power infrasound pulses. Using a family of unmatched filters, the accuracy of the localization can be significantly improved without increasing the power of source pulses. Limiting pulse power has great importance when exploration is performed by autonomous robots (Morris et al., 2006) with limited energy source or usage of higher energy pulses is not desirable (e.g. in order to stay undetected in hostile environment).

2 MAXIMUM LIKELIHOOD MATCHED FILTER ESTIMATOR

In remote sensing applications such as radar or sonar, the common scenario starts by a transmitter sending out a pulse waveform $\mathbf{s}(t)$. The pulse is reflected from a target and it is picked up by a receiver at time \mathbf{t}_0 . The estimated two-way travel time (lag) can be used to calculate distance to the target assuming the speed of the pulse propagation in the medium is known.

The signal recorded at the receiver might be represented as

$$\mathbf{u}(t) = c * \mathbf{s}(t - \mathbf{t}_0) + \mathbf{n}(t)$$

where $\mathbf{n}(t)$ is Additive White Gaussian Noise (AWGN) which corrupts the signal. The $c < 1$ factor is used to account for all non-free space propagation losses (e.g. attenuation of the signal in the medium). We are interested in estimating the Time of Arrival (ToA) parameter \mathbf{t}_0 under the assumption that noise \mathbf{n} is large relative to $c*\mathbf{s}(t)$.

The standard method for ToA estimation employs Matched Filter (MF) applied to the received signal. The Matched Filter maximizes peak signal to mean noise ratio (Whalen, 1995), making its output suitable for the Maximum Likelihood (ML) estimator of the ToA. The Matched Filter Maximum Likelihood (MFML) estimator of ToA is obtained by taking the position of the global maximum in the

output of the Matched Filter (MF). The output of the Matched Filter can be expressed as a correlation of the signal with the pulse waveform:

$$\mathbf{y}(\mathbf{t}) = \mathbf{u}(\mathbf{t}) \circ \mathbf{s}(\mathbf{t}) = \mathbf{g}(\mathbf{t}) + \mathbf{h}(\mathbf{t})$$

Where $\mathbf{g}(\mathbf{t})$ is scaled and shifted version of the pulse's autocorrelation function and $\mathbf{h}(\mathbf{t})$ is filtered noise. A typical Gaussian-modulated sinusoidal pulse and its autocorrelation function are shown in Figure 1.

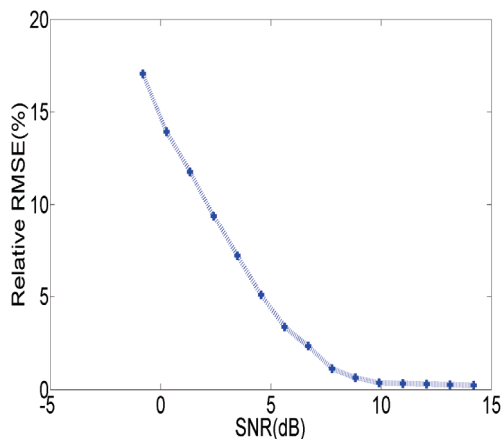


Figure 2: The MFML estimator threshold effect. The error increases rapidly as SNR falls below a threshold.

In the absence of noise, the maximum value of $\mathbf{y}(\mathbf{t})$ is achieved at $\mathbf{t} = \mathbf{t}_o$. As the level of noise increases, the filtered noise $\mathbf{h}(\mathbf{t})$ may cause a slight shift in the location of the peak of $\mathbf{y}(\mathbf{t})$. However, at the high noise levels, a location around one of the side lobes of $\mathbf{g}(\mathbf{t})$ may occasionally become the global maximum of $\mathbf{y}(\mathbf{t})$.

A side lobe of autocorrelation function mistakenly taken as its global maximum is a major reason behind deterioration in accuracy of MFML estimator known as threshold effect (Woodward, 1953). The threshold effect manifests itself in rapid increase in the Root Mean Square Error (RMSE) of the MFML estimator as shown in the Figure 2. In semi-coherent state, the posterior distribution of the possible lag locations becomes multimodal (Figure 3) because of the significant height of autocorrelation function's side lobes.

The height of the side lobes of the autocorrelation function is affected by the pulse bandwidth. Therefore, the threshold effect is considerable for low-frequency narrowband pulses. The analysis of the performance of different time-of-arrival estimation methods is essential for Radar, Sonar and other remote sensing applications. Rather than compute the exact error of a specific estimator,

it is often more convenient to lower-bound the error of any estimators for a given problem.

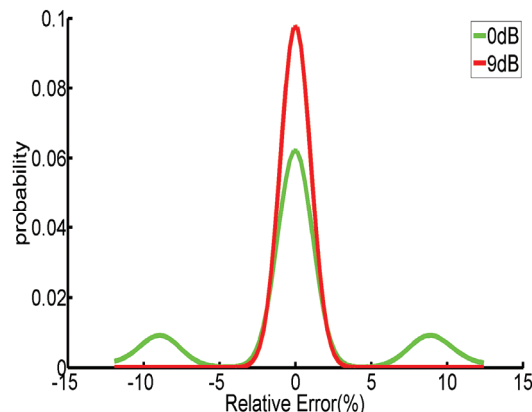


Figure 3: The probability density function for MFML estimator error. There are significant local maxima under low SNR.

The conventional Matched Filter Maximum Likelihood (MFML) estimator is considered efficient as it asymptotically attains the Cramer-Rao Bound (CRB) under sufficiently high SNR conditions (Van Trees, 1968). However, under lower SNR levels, the Cramer-Rao Bound appears to be over-optimistic and a more tight forms of bound are required if the level of noise is high. The Barankin Bound (Barankin, 1949) and associated Barankin Theory provide tools for constructing useful bounds for mean error of an estimator under low SNR. Although in its general form the Barankin bound depends on the estimated parameter and therefore can't be easily computed, it is able to account for the threshold phenomena in the estimation of the time-of-arrival parameter.

3 UNMATCHED FILTER MAXIMUM LIKELIHOOD ESTIMATOR

Given an arbitrary pulse waveform $\mathbf{s}(\mathbf{t})$, we construct a pair of Phase Shifted Unmatched (PSU) filters $\mathbf{f}_\varphi^+(\mathbf{t})$ and $\mathbf{f}_\varphi^-(\mathbf{t})$ by shifting the phase of each pulse by $+\varphi$ and $-\varphi$ respectively. A Gaussian-modulated sinusoidal pulse and its PSU filter pair generated using $\varphi = \pi/2$ are shown in Figure 4.

The cross correlation of the signal $\mathbf{u}(\mathbf{t})$ and a PSU pair's filter can be expressed as:

$$\mathbf{y}_\varphi^\pm(\mathbf{t}) = \mathbf{u}(\mathbf{t}) \circ \mathbf{f}_\varphi^\pm(\mathbf{t}) = \mathbf{g}_\varphi^\pm(\mathbf{t}) + \mathbf{h}_\varphi^\pm(\mathbf{t})$$

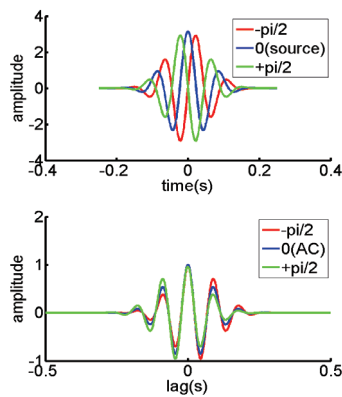


Figure 4: Phase shifted pulses (top) and their cross correlation functions (bottom). Note asymmetric shape of side lobes.

The Unmatched Filter Maximum Likelihood (UFML) estimators t_{φ}^{-} and t_{φ}^{+} corresponding to a PSU pair can be defined as:

$$t_{\varphi}^{\pm} = \underset{t}{\operatorname{argmax}} (y_{\varphi}^{\pm}(t)) = \underset{t}{\operatorname{argmax}} (u(t) \circ f_{\varphi}^{\pm}(t))$$

The side lobes of the cross-correlation function $\mathbf{g}_{\varphi}^{\pm}(\mathbf{x}) = \mathbf{s}(t) \circ \mathbf{f}_{\varphi}^{\pm}(t)$ have unequal heights, making the UFML estimators biased toward the higher side lobe as shown in Figure 5.

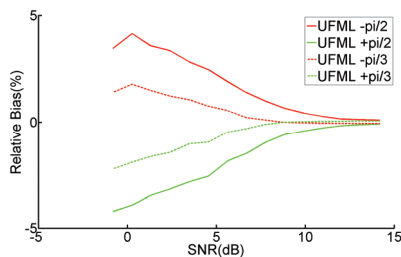


Figure 5: Bias of UFML estimator pair. Unmatched filter pair produces biased estimator pair with bias of the same value but opposite sign.

The bias of the two UFML estimators has equal absolute value but opposite sign due to symmetry in the heights and position of the cross-correlation side lobes. As SNR is increased, the bias decreases since the position of the cross-correlation maximum is less affected by the noise. Note that autocorrelation and PSU filter cross-correlation produce signals of the same power, however application of unmatched filter produces lower peak signal-to-mean-noise ratio as compared to matched filter.

The Root Mean Square Error (RMSE) of a single UFML estimator is higher as compared to the RMSE of MFML. However, the UFML estimators corresponding to a PSU filter pair are not perfectly correlated.

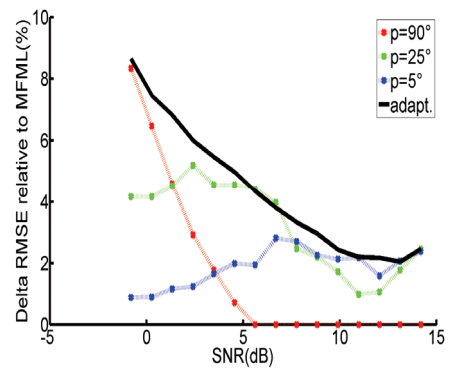


Figure 6: RMSE improvement by fixed and adaptive phase AoUFML estimators. For each SNR there is the best performing value of a phase shift (color lines). The black line shows error for adaptive selection of phase-shift value.

Therefore we can define a new estimator by averaging results from a pair of UFML:

$$t_{\varphi} = \frac{t_{\varphi}^{-} + t_{\varphi}^{+}}{2}$$

At low SNR levels, the resulting Average of UFML (AoUFML) estimator has lower RMSE as compared to MFML (Figure 6).

The AoUFML estimator outperforms MFML estimator at SNR levels corresponding to semi-coherent receiver state. At higher SNR levels, the effect of side lobes is insignificant, therefore, the shape of the main peak of cross-correlation function have critical impact on the estimator's RMSE. Since an unmatched filter produces smaller peak signal-to-mean-noise ratio and the UFML pair is almost perfectly correlated at higher SNR levels, the MFML estimator outperform the AoUFML estimator t_{φ} at coherent receiver state.

The crossover points between AoUFML and MFML RMSE curves can be controlled by choosing appropriate phase shift parameter φ as described in (Apartsin et al., 2010). Finally, we note that many of the commonly used source waveforms have side lobes in their autocorrelation function (e.g. Ryan, 1994). Therefore, although the effectiveness of the proposed method is demonstrated using Gaussian-modulated sinusoidal pulse, the method can be applied to other source waveforms as well.

4 2D SOURCE LOCALIZATION

The described method can be used for the localization of reflection source in 2D or 3D seismic/acoustic maps. Using sensor arrays, a 2D or

3D image of the underground can be computed. On the computed map we might want to pinpoint the location of specific features and voids like a “box” feature shown at Figure 7(left).

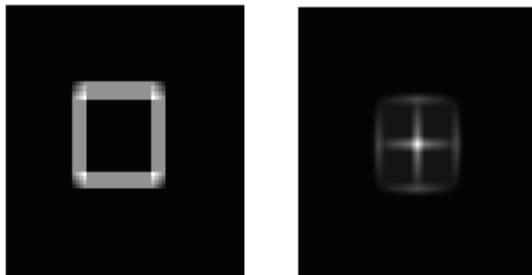


Figure 7: *Left*: Density map of a “box” feature (void), *Right*: 2D autocorrelation function, lighter points corresponds to larger values. There are 4 local peaks in autocorrelation function corresponding to 4 edges of the box.

If underground exploration is performed using low power low frequency seismic pulses, the resulting image would be heavily corrupted by noise. As in one-dimensional case, the estimation of a feature position using conventional matched filters or 2D template would suffer from the threshold effect due to existence of 4 local peaks in the feature’s 2D autocorrelation function (Figure 7 right). Again, instead of relying on a correlation with a single matched filter, the family of 2D unmatched filters using a phase shift can be generated.

Unlike the one-dimensional case, in 2D we have greater choice of phase directions. It seems reasonable to choose phase shift values in the direction of local peaks of the autocorrelation functions. For “box” feature it translates into the vertical and horizontal directions of phase shift. This choice of directions corresponds to the family of 4 unmatched filters (two members of this family are shown at Figure 8). Estimators corresponding to each unmatched filter are biased toward one of the two local maxima in the direction of the phase shift. However, the estimators are not completely correlated as in one dimensional case.

Therefore, by averaging the position of the peaks obtained by cross-correlating noisy map image with filters from the constructed filter family, the accuracy of the position estimation (localization) of the feature is significantly improved (Figure 9). For features with more complex configuration the number of filters can be increased even further to account for all of local maxima in autocorrelation function.

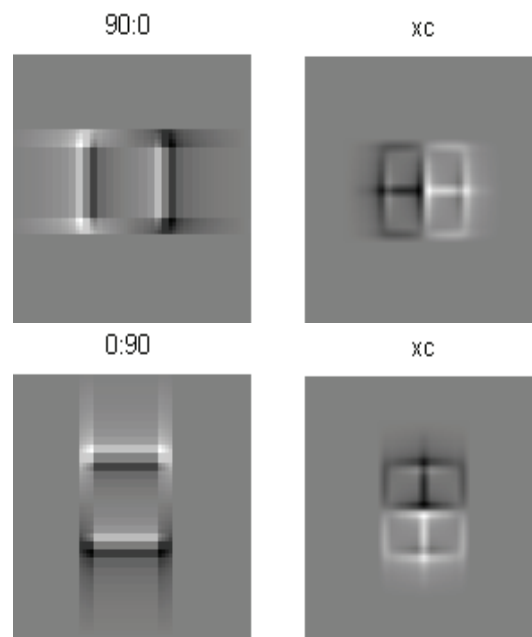


Figure 8: Phase-shifted 2D filters (left column) and their cross-correlation with “box” feature (right column) for horizontal (top row) and vertical (bottom) phase shift directions.

5 CONCLUSIONS

Inspired by the capability of blind mole rat to cope with the threshold effect while exploring underground using low-power low-frequency pulses, we suggest a method for robust time of arrival estimation and 2D source localization and template matching.

We showed that using Phase Shifted Unmatched (PSU) filters, a pair of Unmatched Filter Maximum Likelihood (UFML) estimators can be computed to obtain biased Time of Arrival estimators. In semi-coherent receiver state, the UFML estimators are not perfectly correlated and, therefore, can be combined together into estimator that outperforms conventional Matched Filter Maximum Likelihood estimator.

The described method can be applied for 2D source localization using a family of Unmatched Filters generated by phase shifting original template in multiple directions. The method can be applied for underground exploration and mapping using low power low frequency seismic signals.

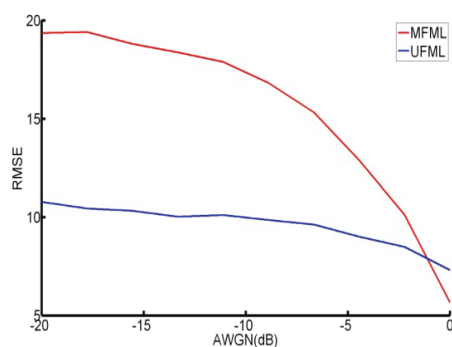


Figure 9: RMSE as function of SNR Using fusing from 4 estimators (2 horizontal phase shift and 2 vertical phase shift) gives higher accuracy than conventional matched-filter approach.

REFERENCES

- Apartsin, S. Cooper, L. N. and Intrator, N., 2010. *SNR-Dependent Filtering for Time of Arrival Estimation in High Noise*. To appear in Proc. IEEE Int. Workshop on Machine Learning for Signal Processing (MLSP).
- Barankin, E. W., 1949. *Locally best unbiased estimates*. Ann Math. Statist., 20, pp477-501.
- Kay, S. M., 1993. *Fundamental of Statistical Signal Processing*. Prentice Hall.
- Kimchi, T., Reshef, M. and Terkel, J., 2005. *Evidence for the use of reflected self-generated seismic waves for spatial orientation in a blind subterranean mammal*. Journal of Experimental Biology, vol208, pp647-658.
- Liao, H. S. and Gan, L. and Wei, P., 2009. *A blind SNR estimation method for radar signal*. IET international RADAR conference.
- McDonough, R. N., Whalen, A. D., 1995. *Detection of Signals in Noise*. Academic Press.
- Morris, A. and Ferguson, D. and Omohundro, Z., Bradley, D., Silver, D., Baker, C., Thayer, S., Whittaker, C. and Whittaker, W., 2006. *Recent developments in subterranean robotics*. Journal of Field Robotics, 23(1), 35-57.
- Pauluzzi, D. R., Beaulieu N. C., 2000. *A comparison of SNR estimation techniques for the AWGN channel*. IEEE Transaction on Communications. Volume 48, Issue 10, pp1681-1691.
- Ryan, H., 1994. *Ricker, Ormsby, Klauder, Butterworth-A choice of wavelet*. CSEG Recorder, Vol. 19-7.
- Sadler, B. M., Kozick, R. J., 2006. *A Survey of Time Delay Estimation Performance Bounds*. Fourth IEEE Workshop on Sensor Array and Multichannel Processing, pp.282-288.
- Skolnik, M. I., 1962. *Introduction to Radar Systems*. McGraw-Hill.
- Succi, G. P., Prado, G., Gampert, R. and Pedersen, T. K., 2000. *Problems in Seismic detection and Tracking*. Proceedings of SPIE, vol. 4040, pp165-173.
- Woodward, P., 1953. *Probability and Information Theory, with Applications to Radar*. McGraw-Hill.

- Van Treese, H. L., 1968. *Detection, Estimation and Modulation Theory*. John Wiley & Sons, Inc.
- Varshney, L. R., Thomas, D., 2003. *Sidelobe reduction for matched filter range processing*. Proceedings of IEEE Radar Conference, pp446-451.
- Yu, L., Neretti, N. and Intrator, N., 2006. *Multiple ping sonar accuracy improvement using robust motion estimation and ping fusion*. Journal of the Acoustic Society of America. Volume 119, Issue 4, pp2106-213.
- Zeira A. and Schultheiss, P. M., 1994. *Realizable lower bounds for time delay estimation-Part II: Threshold phenomena*. IEEE Trans. Signal Processing, Volume42, Issue 5, pp1001-1007.